coatings

MDPI

Article

Oxygen Interactions with Covalently Grafted 2D Nanometric Carboxyphenyl Thin Films—An Experimental and DFT Study

Veton Haziri [1,2], Sereilakhena Phal [3], Jean-François Boily [3], Avni Berisha [1,4,*] and Solomon Tesfalidet [3,*]

1 Department of Chemistry, University of Prishtina, 10000 Prishtina, Kosovo; veton.haziri@ubt-uni.net
2 Department of Food Science and Biotechnology, UBT College, 10000 Prishtina, Kosovo
3 Department of Chemistry, Faculty of Science and Technology, Umeå University, 901 87 Umeå, Sweden; phal.sereilakhena@gmail.com (S.P.); jean-francois.boily@umu.se (J.-F.B.)
4 Materials Science—Nanochemistry Research Group, NanoAlb—Unit of Albanian Nanoscience and Nanotechnology, 1001 Tirana, Albania
* Correspondence: avni.berisha@uni-pr.edu (A.B.); solomon.tesfalidet@umu.se (S.T.)

Abstract: Surface modification is a hot topic in electrochemistry and material sciences because it affects the way materials are used. In this paper, a method for covalently attaching carboxyphenyl (PhCOOH) groups to a gold electrode is presented. These groups were grafted onto the electrode surface electrochemically via reduction of aryldiazonium salt. The resulting grafted surface was characterized using cyclic voltammetry (CV) before and after the functionalization procedure to validate the presence of the grafted layer. The grafting of PhCOOH groups was confirmed by analyzing electrode thickness and composition by ellipsometry and X-ray photoelectron spectroscopy (XPS). Density functional theory (DFT) calculations indicated that the grafted layers provide a stable platform and resolved, for the first time, their interactions with oxygen.

Keywords: nanometric thin films; grafting; cyclic voltammetry; DFT; PhCOOH

Citation: Haziri, V.; Phal, S.; Boily, J.-F.; Berisha, A.; Tesfalidet, S. Oxygen Interactions with Covalently Grafted 2D Nanometric Carboxyphenyl Thin Films—An Experimental and DFT Study. *Coatings* **2022**, *12*, 49. https://doi.org/10.3390/coatings12010049

Academic Editor: Cheng Zhang

Received: 19 November 2021
Accepted: 28 December 2021
Published: 1 January 2022

1. Introduction

The use of aryl radicals, formed during the dediazotization of aryldiazonium salts, to modify/functionalize various surfaces is regarded as a simple and resourceful tool [1]. In contrast to other surface modification methods (thiols, phosphonic acids, etc.) [2], electrografting remains the most efficient way to modify surfaces, regardless of the surface type (metal, semiconductor, or insulator). Despite the fact that the structure of the surfaces, grafted with aryl layers, has been thoroughly investigated experimentally using a variety of experimental techniques such as XPS, Raman, infrared reflection-absorption spectroscopy (IRRAS), atomic force microscopy (AFM), as the interaction of oxygen, with this interface remains unexplored.

The majority of research has deemed diazonium salts to be simple and effective coupling agents between the surface and other functional entities. For instance, grafted layers have been used to attach nanoparticles [3,4], proteins [5], calixarenes [6], polymers [7,8], and DNA [5,9]. Another significant aspect that makes this approach attractive for surface modification processes is the stability of the nanocomposite structure formed once the aryl moieties are attached to the electrode surface [10]. Grafted surfaces have found a vast number of practical applications in biomedicine, microfluidics, sensors, biosensors, corrosion protection, and energy conversion [11].

In this study (Scheme 1), the interaction of oxygen with 2D carboxyphenyl (CP) layers grafted onto gold was explored experimentally and by molecular modeling. In general, oxygen bubbles and microbubbles are interesting prospects for future practical applications, and they allow exploration of the electrical characteristics of the gas–water interface using different analytical approaches. They are engaged in several activities, including photo-assisted water splitting reactions [12,13], in the fabrication of gas-sensing electrodes [14,15],

foam fractionation [16,17], food processing [18], and purification processes [19]. Thus, understanding the interaction of oxygen with modified electrode surfaces is essential for developing these various applications.

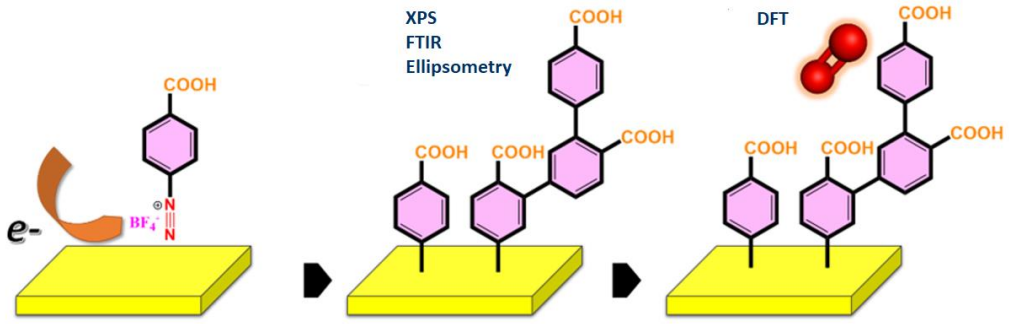

Scheme 1. The surface modification of Au with PhCOOH layers and the interaction of the generated interface with molecular oxygen are depicted schematically. The techniques used include XPS, Fourier-transform infrared spectroscopy (FTIR,) and ellipsometry for surface characterization and DFT for modeling the interaction of molecular oxygen with the grafted surface.

2. Materials and Methods

Pressure-fit gold discs with a diameter of 1.5 mm were inserted into insulating Teflon sleeves to create the Au electrode. Tetrabutylammonium tetrafluoroborate (NBu_4BF_4), 4-aminobenzoic acid, absolute ethanol (spectroscopy grade, 99.9%), potassium chloride, sodium hydroxide, sodium nitrite ($NaNO_2$), tetrafluoroboric acid (HBF_4), diethyl ether, potassium ferrocyanide ($K_4[Fe(CN)_6]\cdot 3H_2O$), potassium ferricyanide, and HPLC-grade acetonitrile (ACN) were acquired from Fisher Scientific (Bishop Meadow, Loughborough, UK).

2.1. Preparation of 4-Carboxybenzenediazonium Tetrafluoroborate

A diazotization procedure was used to produce the 4-carboxybenzene diazonium salt (4-CBD) in situ [20]. In brief, 4-aminobenzoic acid (35 mmol) was dissolved in a mixture of 10 mL HBF_4 and 10 mL H_2O. Under constant stirring, the solution mixture was transferred to an ice bath. After roughly a half hour, a solution of $NaNO_2$ (37 mmol) was added, yielding the final product. The precipitate was rinsed with diethyl ether and vacuum-filtered before storage at −20 °C in the dark. Fourier-transform infrared (FTIR) spectroscopy analysis of the resulting 4-carboxybenzenediazonium tetrafluoroborate (4-CBD) was compared with the spectra of 4-aminobenzoic acid (parent compound). Spectra were collected in the 600–4000 cm^{-1} region in attenuated total reflectance (ATR) mode using a Vertex 60/v spectrometer (Bruker, Billerica, MA, USA).

The resulting 4-CBD was also characterized by cyclic voltammetry (CV). For this experiment, 2.5 $mmol\cdot L^{-1}$ of 4-carboxybenzenediazonium tetrafluoroborate in ACN containing 50 $mmol\cdot L^{-1}$ of NBu_4BF_4 was utilized. CVs were recorded in the +0.5 to −0.3 V range at v = 100 mV/s.

2.2. Modification of Au Electrode

The Au electrode was polished with 1.0 micron alumina slurry (Buehler, Esslingen, Germany) and washed with Q-POD®'s Milli-Q water (Merck, Darmstadt, Germany,) water before the modification. It was sonicated for 5 min with ethanol and then with water to eliminate any remaining impurities. The electrode was then cleaned electrochemically in 0.5 M H_2SO_4 by running 25 cycles of CV at 100 mV/s in the range of −0.3 to 1.5 V until a repeatable voltammogram was obtained.

Chronoamperometry was used to graft the gold electrode surface, which was conducted at −0.3 V vs. Ag/AgCl (saturated KCl) reference electrode for 600 s in a solution of 2.5 mmol/L 4-carboxybenzene diazonium tetrafluoroborate containing 50 mmol/L

NBu_4BF_4 in ACN. The grafted electrode was then rinsed with Milli-Q water, sonicated for about 200 s in acetonitrile, and then rinsed again with Milli-Q water.

2.3. Molecular Modeling

Density functional theory (DFT) calculations were made to elucidate the interaction of molecular oxygen with the Au (111) surface, grafted with carboxyphenyl groups. These calculations were made using a generalized gradient approximation (GGA) [21]/double-numeric polarized basis set (DND) using a four-layer model under the following periodic boundary conditions. Cell dimensions were 9.99 Å × 9.99 Å × 7.951 Å (with the addition of a 20 Å vacuum layer along the *c* axis) grafted with carboxyphenyl groups. The van der Waals interactions were included using the Tkatchenko–Scheffler (TS) method [22]. The interaction of the oxygen molecules (in vacuum and water using the conductor-like screening model) [23–25] with the bare and grafted gold surfaces was evaluated at different reaction sites. The results gave important molecular insight into the adsorption energy and geometry-induced changes brought about by the interaction of oxygen molecule on the grafted interface [26].

Gaussian 16 was used for the calculations on Au clusters. A gold (Au20) cluster was used to model the grafting of Au20−PhCOOH and its interaction with molecular oxygen [27]. The DFT geometry optimizations (executed without symmetry constraints) were accomplished using Grimme's dispersion correction at the B3LYP level of theory (GD3).

The aug-cc-pvdz basis set was used to describe C, H, and O atoms, whereas the LanL2DZ basis set was used for gold atoms. The integral equation formalism polarizable continuum model (IEFPCM) was applied to account for water as solvent in the DFT calculations. All energy minima were characterized with a vibrational analysis to ensure the lack of imaginary frequencies [28]. Noncovalent interaction (NCI) surface plots were generated using Multiwfn and VMD (Visual Molecular Dynamics, version 1.9.4a51) software [29,30]. The bond dissociation energy (BDE) was calculated as [27,28]:

$$BDE_{(Au\text{-}PhCOOH)} = (E_{PhCOOH} + E_{Au}) - (E_{Au-PhCOOH})$$

where $E_{Au\text{-}PhCOOH}$ is the total energy of the Au surface grafted by a –PhCOOH moiety, and E_{PhCOOH} and E_{Au} represent the energies of the isolated Au and PhCOOH entities, respectively.

2.4. Ellipsometry

The thickness of the film and its refractive index were determined using an alpha-SETM ellipsometer (J.A. Woollam Co., Inc., Lincoln, NE, USA). The measurements were performed at a 70° incidence angle. Ellipsometric measurements were taken before and after electrografting on the identical region of the sample plates. The optical thickness was estimated using a built-in model (CompleteEASE). The bare-gold and grafted-gold electrodes were modelled using the B-spline and WvlByWvl models, respectively.

2.5. X-ray Photoelectron Spectroscopy (XPS)

The XPS spectra for the grafted gold plates were obtained using a Kratos Axis Ultra DLD electron spectrometer (Kratos Analytical Ltd, Manchester, UK) equipped with a monochromated Al Ka source operating at 150 W. Survey spectra were obtained at binding energies ranging from 1100 eV to 0, with a pass energy of 160 eV and high-resolution spectra of the major photoelectron lines C 1s and O 1s at a pass energy of 20 eV. The spectra were processed using the Kratos Vision 2 program (version 2.2.9).

3. Results and Discussion

3.1. Characterization of Synthesized Diazonium Salt Using FTIR

The IR spectra (registered using Bruker IFS 66 v/S FTIR spectrometer with a 2 cm^{-1} resolution and plotted by OriginPro 2021 software, version 9.8.0.200 of the synthesized diazonium salt were used to confirm its identity. New functional groups were identified in the IR spectra at 2285 cm^{-1} and 1112–1034 cm^{-1}, corresponding to −N≡N+ [20,31]

and BF_4^-, respectively. These signals are obviously absent in the parent molecule (4-aminobenzoic acid).

Furthermore, when compared with the N–H groups in 4-aminobenzoic acid, the intensities of the N–H groups in the product were lower, and the wavenumber was displaced (Figure 1). These findings confirm that the 4-carboxybenzenediazonium tetrafluoroborate salt was successfully synthesized.

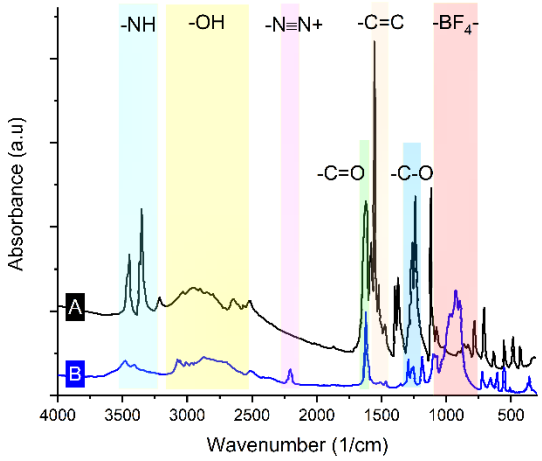

Figure 1. IR spectra of (**A**) 4-carboxybenzenediazonium tetrafluoroborate and (**B**) 4-aminobenzoic acid.

3.2. Characterization of the Electrode Modification Steps

Modification of Au Electrode by Chronoamperometry

The current decreases as the Au electrode is modified using chronoamperometry, implying the creation of a relatively thick layer of carboxyphenyl layer on the surface. The chronoamperogram (Figure 2) had the same characteristics as the grafting of multilayer films from different aryl diazonium salts [32], with an instant drop in the current during the first 100 s, after which it remained constant due to electrode blocking by the grafted layer.

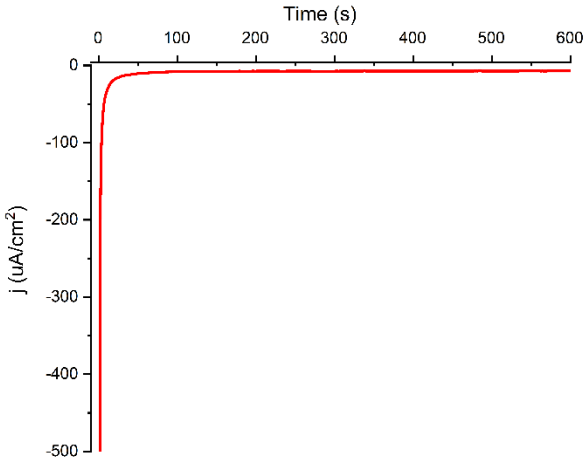

Figure 2. Chronoamperometry of 4-aminobenzoic acid with $NaNO_2$. Potential peak −0.6 V and the reduction time 600 s.

3.3. Characterization of the Synthesized Diazonium Salt Using CV

The CV scans obtained during the grafting of the 4-CBD are shown in Figure 3. The current reduction, observed in the subsequent CV scans, confirms the deposition of a cabocyphenyl layer on the electrode surface [33,34].

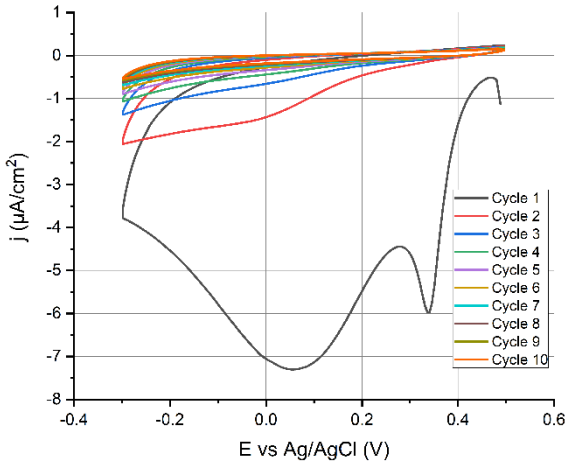

Figure 3. CV of 2.5 mmol·L^{-1} 4-CBD +50 mmol·L^{-1} NBu4BF4; v = 100 mV/s and voltage range +0.5 to −0.3 V.

This indicates that the electron transfer blocking characteristics of the grafted layer prevented further electrochemical reduction of diazonium. Very sharp peaks occurred at 0.34 and 0.062 V vs. ref. These two reduction peaks were most likely caused by diazonium reduction on unique crystallographic orientations of the polycrystalline gold surface [35]. The 0.062 V vs. ref peak, however, vanished in successive CV cycles (Figure 3).

3.4. Cyclic Voltammetry with the Redox Probe, Fe (CN)$_6^{3-/4-}$

Figure 4 shows the CV obtained for the redox probe using the bare Au electrode and the modified electrode. The voltammogram of a bare Au electrode shows a well-defined Fe(CN)$_6^{3-/4-}$ oxidation/reduction peak, indicating a quasi-reversible redox activity. After the deposition of the 4-carboxyphenyl layer (CP), the current decreased and widened the peaks. The current reduction is due to the creation of partially blocking organic layers [36].

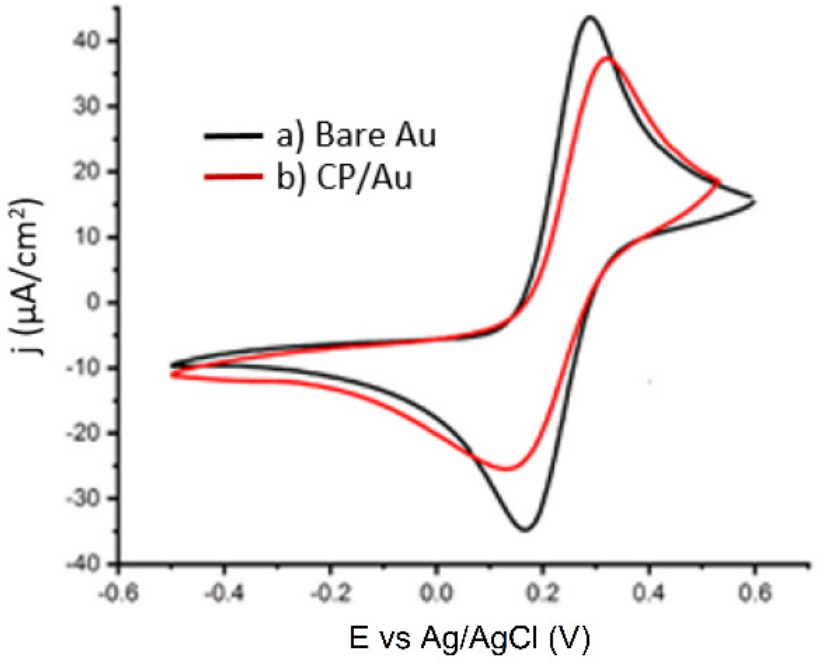

Figure 4. CV of 5.0 mmol·L^{-1} Fe(CN)$_6^{3-/4-}$ containing 100 mmol·L^{-1} KCl: **a**) bare Au, **b**) CP/Au.

3.5. XPS Characterization of Au-CP

Changes in the surface compositions of the bare and grafted gold electrode were detected by XPS (Table 1). The bare gold surface contained carbon impurities, such as aliphatic carbon (28.99 at.%) and carboxyl and carbonyl groups seen in the C 1s and O 1s regions. The grafted electrode, however, had greater loadings of carbon species resulting from the PhCOOH coatings. This can first be appreciated by the loss in the Au peak, decreasing from 54.79 at.% in the bare gold surface down to 44.37 at.% in the grafted electrode.

Table 1. Atomic concentrations (AC) (in.%) of various elements on the surface of a modified gold electrode.

Signal	BE, eV	AC, at.%	at.% per Au	BE, eV	AC, at.%	pat.% Per Au	Bond Type
-	Bare Au		-	CP/Au		-	
C 1s	284.2	28.99	0.53	284.5	30.98	0.70	C–(C,H)
-	285.8	4.94	0.090	285.9	6.56	0.15	C–OH, C–O–C
-	287.1	2.89	0.053	287.1	2.91	0.066	C=O
-	288.5	1.4	0.026	288.4	3.71	0.084	COOH
O 1s	530.8	4.26	0.078	530.7	2.77	0.062	C=O
	-			531.8	6.38	0.144	COOH
-	532.4	2.73	0.050	533.1	2.34	0.053	C–OH
Au 4f 7/2	84	54.79	1.00	0.65	44.37	1.00	-

For the grafted layer, compared to the bare, an increase in the content of carbon and oxygen (per Au) was observed throughout the C 1s and the O 1s regions: e.g, increase from 0.53 to 0.70 in C–(C,H), from 0.090 to 0.15 in C–OH/C–O–C, and from 0.026 to 0.084 in COOH. The O 1s region corroborates with the hike in carbon-bound oxygen species, with the appearance of a new peak at 531.8 eV from COOH functional groups. These findings confirm the coating of PhCOOH on the electrode surface.

3.6. Ellipsometry

The ellipsometric measurements were performed before and after electrografting of PhCOOH on the gold plates. The measurements were made on dried and hence collapsed films. The layer's refractive index was therefore set to a constant value (real = 1.50; imaginary = 0), regardless of its thickness. The thickness of the deposited layer, estimated using the average of five separate measurements, was found to be 1.9 ± 0.35 nm. Taking into account that the thickness of one PhCOOH moiety is ≈0.518 nm (modelled, optimized, and measured using Avogadro software, version 1.2.0), our film is a multilayer (≈3.6 layer thick).

3.7. DFT Calculation

Bond dissociation energy (BDE) is widely used to evaluate the stability of diazonium salt-grafted layers [25–28]. The computed BDE for the carboxyphenyl group was −52.19 kcal/mol. These values are indicative of a stable interface formation.

The interaction of oxygen molecules with the gold surface's grafted layers (Ph-COOH) was also investigated. Four distinct initial geometries were explored to investigate the interaction between the grafted Au-PhCOOH surface and molecular oxygen (as presented in Figure 5). The interaction of oxygen molecules with the grafted surface causes structural changes in all geometries, but especially when the molecule is closer to the phenyl ring's side. This is probably related to electron-rich aromatic ring and oxygen lone pairs that ex-

hibit attractive interactions [37]. The carboxyphenyl layer exhibits the strongest interactions at the bridge (BRD) position (Table 2), with an interaction energy of −228.86 kJ/mol.

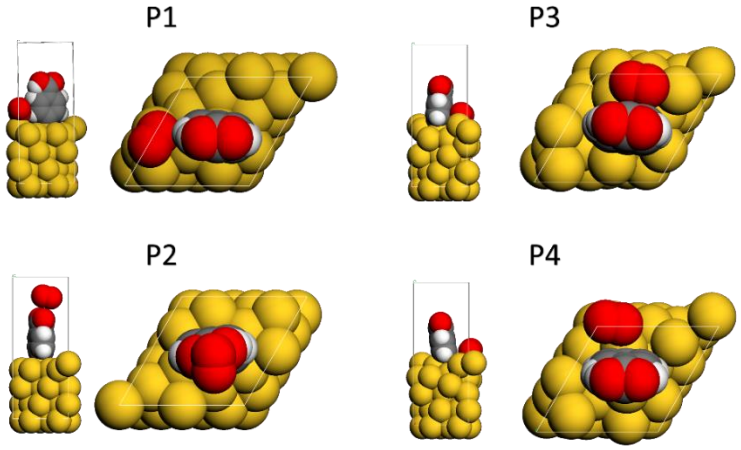

Figure 5. Optimized geometries of the oxygen molecule: (**P1**) on top of the Au surface, (**P2**) on top of the attached Ph-COOH moiety, (**P3**) bridge on the Au surface, (**P4**) fcc-hollow (level of theory: GGA/DND/TS).

Table 2. BDE for different optimized energies of oxygen molecules interacting on the grafted gold surfaces (level of theory: GGA/DND/TS).

Position	BDE (kJ/mol)
P1	−53.55
P2	−228.86
P3	−182.84
P4	−61.50

According to Figure 6a,b, the BDE values for Au-2PhCOOH were higher compared with the BDE values for Au-PhCOOH. This is consistent with the findings of De-en Jiang et al. and Haziri et al. [38,39], who demonstrated that the inclusion of the second grafted group enhances the bond's stability.

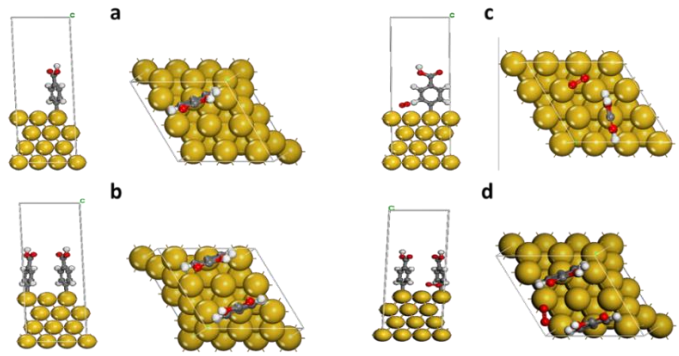

Figure 6. Optimized geometries of gold surfaces grafted with carboxyphenyl groups in absence and presence of oxygen molecule (level of theory: GGA/DND/TS). (**a**) Au-CP; (**b**) Au-CP/O_2; (**c**) Au-2CP; (**d**) Au-2CP/O_2.

DFT calculations were used to investigate the potential of a gold surface, grafted with a film of PhCOOH, to adsorb oxygen molecules at the molecular level. The calculated values were then used to determine the binding energy for the adsorption of molecular oxygen on the carboxyphenyl molecule grafted on the gold cluster (Figure 7A,B).

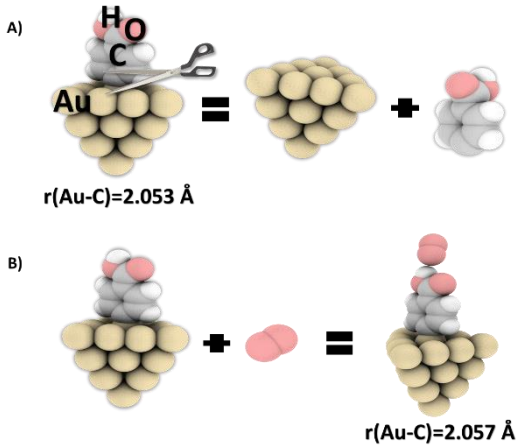

Figure 7. (**A**) Bond dissociation energies (calculated by DFT) for a Au cluster with grafted carboxyphenyl moieties and (**B**) optimized structures for the interaction of oxygen molecules with the Au-PhCOOH system (level of theory: DFT/B3LYP/aug-cc-pvdz for C, H, and O atoms and LanL2DZ basis set for Au atoms).

These results provide new information on the layers' ability to interact with oxygen molecules. The Au–C bond formed between PhCOOH and Au20 was 2.053 and 2.057 Å before and after the interaction with oxygen molecule, respectively. After grafting, the gold atom was drawn out from the mean surface plane of the Au20 cluster by about 0.479 Å. This distance increased to 0.51 Å in the presence of molecular oxygen, which can weaken the Au–C bond. Additional calculations were also performed on the geometric structure of the gold cluster after grafting and interaction with oxygen molecules. Angles between the PhCOOH ring and the Au surface were of 89.9° in the O_2-free and 80.0° in the O_2-bearing systems [27].

To understand the adsorption details of the oxygen molecule onto the bare and CP-grafted gold surface, the NCI 2D and 3D plots [40,41] for the interaction of O_2 molecule with both surfaces were computed (Figure 8). The result confirms that adsorption proceeds through van der Waals interactions (cf. green color on the surface, spikes at −0.01 to −0.04 on the 2D plot).

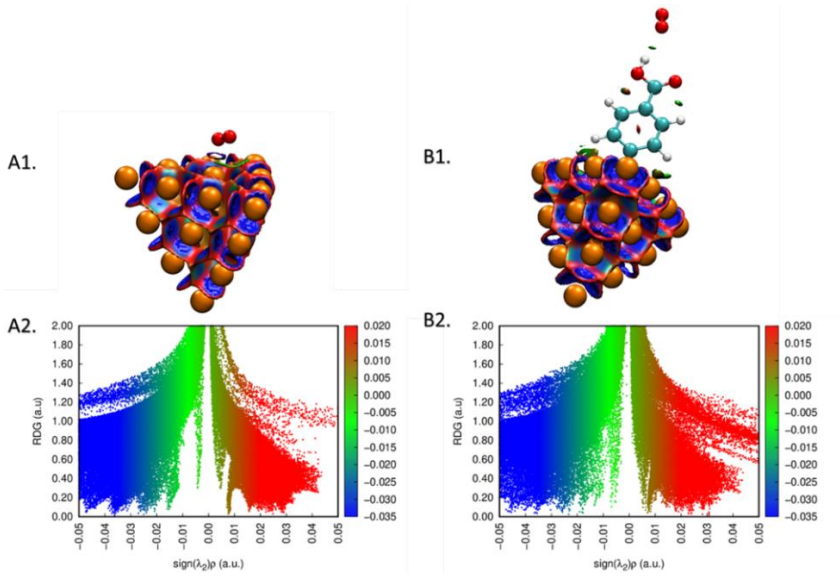

Figure 8. (**A1**,**B1**) Noncovalent interaction surfaces and the plot of (**A2**,**B2**) reduced density gradient (RDG) vs. sign(λ)ρ for the interaction of oxygen with bare and Au20-CP cluster.

The bond dissociation energy (BDE) [25,27,40,42], reported in Tables 3 and 4, was used as an indirect measure of the stability of the grafted layers. In comparison with previously described surface modification procedures, based on the creation of self-assembling monolayers (SAM) through thiol chemistry (BDE | Au–S–$(CH_2)_5$–COOH | = 132.21 kJ/mol), the layers formed by grafting diazonium salts were more stable. Their bond dissociation energies were found to be equivalent to those of their thiol analogs.

Table 3. BDE and adsorption energy of oxygen molecule on Au after grafting with two CP groups (level of theory: GGA/DND/TS).

System	BDE (kJ/moL)	Adsorption Energy of the O_2 Molecules (kJ/moL)
Au-PhCOOH	−101.54	-
Au-2PhCOOH	−117.15	-
Au-PhCOOH/O_2	-	−181.04
Au-2PhCOOH/O_2	-	−175.14

Table 4. BDE values of the grafted moieties on different surfaces.

Surface	Grafted Moiety	BDE (kJ/moL)	Reference
Gold cluster	–C_6H_5	143.93	[42]
-	–S–C_6H_5	136.39	-
Pristine graphene sheet (with a grafted phenyl group)	–C_6H_5	-	[39]
Au(111)	–$CH_2(CH_2)_3$COOH	154.39	[27]
Gold cluster (Au10)	-triazole	234.30	[26]
Zigzag SWCN (8.0)	–C_6H_5–Br	293.29	[43]
Zigzag SWCN (13.0)	-	204.51	
Graphyne	–C_6H_5	276.14	[40]
Graphene oxide	–C_6H_5	276.18	[25]
Borophene	–C_6H_5	317.77	[28]
Au(111)	–C_6H_5COOH	101.54	This paper
Au(111)	–2C_6H_5COOH	117.15	This paper

4. Conclusions

To our knowledge, this is the first reported study to address the problem of oxygen adsorption onto grafted layers derived from aryldiazonium salts. This is important as studies have shown that the oxygen content on the interface decreases the grafting efficiency of the generated aryl radicals. Prior to the grafting reaction, deoxygenation with bubbling nitrogen, helium, or argon usually reduces the presence of oxygen in the grafting solution. The electrografting of carboxyphenyl thin films derived from the suitable aryldiazonium tetrafluoroborate salt is demonstrated in this work. CV experiments on the grafted carboxyphenyl layer using $Fe(CN)_6^{3/4-}$ as a redox probe revealed that the layer exhibits partial electron transfer blocking properties. The film was relatively thin, as shown by ellipsometry. XPS confirmed the grafted surface's composition. DFT calculations also shed light on how oxygen interacts with the bare and the CP-grafted gold surfaces. According to NCI, the oxygen molecule interacts with the bare or grafted Au-CP surfaces via van der Waals interactions. The interaction energy gets bigger as the surface coverage of the CP groups increases.

Author Contributions: Conceptualization, A.B.; investigation and experiments, V.H. and S.P.; writing—original draft preparation, A.B., J.-F.B. and S.T.; writing—review and editing, A.B., J.-F.B. and S.T. All authors have read and agreed to the published version of the manuscript.

Funding: This research received no external funding.

Institutional Review Board Statement: Not applicable.

Informed Consent Statement: Not applicable.

Data Availability Statement: Data sharing is not applicable to this article.

Acknowledgments: A.B. acknowledges support from the Ministry of Education, Science, and Technology of Kosovo (Nr.2-5069). V.H. acknowledges support from Erasmus Plus (project: development of an advanced and applied course in electrochemistry with flexible and creative learning). J.-F.B. was supported by the Swedish Research Council (2017-03808; 2020-04853).

Conflicts of Interest: The authors declare no conflict of interest.

References

1. Berisha, A.; Chehimi, M.M.; Pinson, J.; Podvorica, F.I. Electrode surface modification using diazonium salts. In *Electroanalytical Chemistry*, 1st ed.; Bard, A.J., Zoski, C.G., Eds.; CRC Press: London, UK, 2015; pp. 115–224.
2. Love, J.C.; Estroff, L.A.; Kriebel, J.K.; Nuzzo, R.G.; Whitesides, G.M. Self-assembled monolayers of thiolates on metals as a form of nanotechnology. *Chem. Rev.* **2005**, *4*, 1103–1170. [CrossRef] [PubMed]
3. Gehan, H.; Fillaud, L.; Felidj, N.; Aubard, J.; Lang, P.; Chehimi, M.M.; Mangeney, C. A general approach combining diazonium salts and click chemistries for gold surface functionalization by nanoparticle assemblies. *Langmuir* **2010**, *6*, 3975–3980. [CrossRef]
4. Mohamed, A.A.; Salmi, Z.; Dahoumane, S.A.; Mekki, A.; Carbonnier, B.; Chehimi, M.M. Functionalization of nanomaterials with aryldiazonium salts. *Adv. Colloid Interface Sci.* **2015**, *225*, 16–36. [CrossRef] [PubMed]
5. Abdellaoui, S.; Corgier, B.C.; Mandon, C.A.; Doumèche, B.; Marquette, C.A.; Blum, L.J. Biomolecules immobilization using the aryl diazonium electrografting. *Electroanalysis* **2013**, *25*, 671–684. [CrossRef]
6. Mattiuzzi, A.; Jabin, I.; Mangeney, C.; Roux, C.; Reinaud, O.; Santos, L.; Lagrost, C. Electrografting of calix [4] arenediazonium salts to form versatile robust platforms for spatially controlled surface functionalization. *Nat. Commun.* **2012**, *3*, 1–8. [CrossRef] [PubMed]
7. Lillethorup, M.; Shimizu, K.; Plumeré, N.; Pedersen, S.U.; Daasbjerg, K. Surface-attached poly (glycidyl methacrylate) as a versatile platform for creating dual-functional polymer brushes. *Macromolecules* **2014**, *47*, 5081–5088. [CrossRef]
8. Mahouche-Chergui, S.; Gam-Derouich, S.; Mangeney, C.; Chehimi, M.M. Aryl diazonium salts: A new class of coupling agents for bonding polymers, biomacromolecules and nanoparticles to surfaces. *Chem. Soc. Rev.* **2011**, *40*, 4143–4166. [CrossRef]
9. Lee, C.S.; Baker, S.E.; Marcus, M.S.; Yang, W.; Eriksson, M.A.; Hamers, R.J. Electrically addressable biomolecular functionalization of carbon nanotube and carbon nanofiber electrodes. *Nano Lett.* **2014**, *4*, 1713–1716. [CrossRef]
10. Berisha, A. Electrografting and Photografting of Organic Layers onto Conducting and Semi-Conducting Surfaces. Ph.D. Thesis, Université Pierre et Marie CURIE, Paris, France, 2011.
11. Belmont, J.A.; Bureau, C.; Chehimi, M.M.; Gam-Derouich, S.; Pinson, J. Patents and industrial applications of aryl diazonium salts and other coupling agents. In *Aryl Diazonium Salts: New Coupling Agents in Polymer and Surface Science*, 1st ed.; Chehimi, M.M., Ed.; Willey: Hoboken, NJ, USA, 2012; pp. 309–321.
12. Zhang, J.; Lee, J.; Wang, L.; Zheng, Y.; Wang, W.; Guo, J.; Gao, J. Serial microbubble imaging technology (sMBI) for rapid screening of hydrogen-evolution materials used in photocatalytic water-splitting reactions. *Anal. Methods* **2017**, *9*, 1835–1838. [CrossRef]
13. Zhao, X.; Ren, H.; Luo, L. Gas bubbles in electrochemical gas evolution reactions. *Langmuir* **2019**, *35*, 5392–5408. [CrossRef]
14. Nie, C.; Zeng, W.; Jing, X.; Ye, H. NiO hollow nanospheres with different surface by a bubble-template approach and its gas sensing. *J. Mater. Sci. Mater. Electron.* **2018**, *29*, 7480–7488. [CrossRef]
15. Berneschi, S.; Farnesi, D.; Cosi, F.; Conti, G.N.; Pelli, S.; Righini, G.C.; Soria, S. High Q silica microbubble resonators fabricated by arc discharge. *Opt. Lett.* **2011**, *36*, 3521–3523. [CrossRef] [PubMed]
16. Hofmann, A.; Schembecker, G.; Merz, J. Role of bubble size for the performance of continuous foam fractionation in stripping mode. *Colloids Surf. A Physicochem. Eng. Asp.* **2015**, *473*, 85–94. [CrossRef]
17. Burghoff, B. Foam fractionation applications. *J. Biotechnol.* **2012**, *161*, 126–137. [CrossRef]
18. Phan, K.K.T.; Truong, T.; Wang, Y.; Bhandari, B. Nanobubbles: Fundamental characteristics and applications in food processing. *Trends Food Sci. Technol.* **2021**, *95*, 118–130. [CrossRef]
19. Suto, H.; Fujii, S.; Yoshihara, K.; Ishida, K.; Tanaka, Y.; Honda, S.I.; Katayama, M. Fabrication of cold cathode ionization gauge using screen-printed carbon nanotube field electron emitter. *Jpn. J. Appl. Phys.* **2008**, *47*, 2032. [CrossRef]
20. Phal, S.; Shatri, B.; Berisha, A.; Geladi, P.; Lindholm-Sethson, B.; Tesfalidet, S. Covalently electrografted carboxyphenyl layers onto gold surface serving as a platform for the construction of an immunosensor for detection of methotrexate. *J. Electroanal. Chem.* **2018**, *812*, 235–243. [CrossRef]

21. Perdew, J.; Burke, K.; Ernzerhof, M. Generalized gradient approximation made simple. *Phys. Rev. Lett.* **1996**, *77*, 3865–3868. [CrossRef] [PubMed]
22. Tkatchenko, A.; Scheffler, M. Accurate molecular van der Waals interactions from ground-state electron density and free-atom reference data. *Phys. Rev. Lett.* **2009**, *102*, 073005. [CrossRef]
23. Marsh, K.N. *COSMO-RS from Quantum Chemistry to Fluid Phase Thermodynamics and Drug Design*, 1st ed.; Klamt, A., Ed.; Elsevier: Amsterdam, The Netherlands, 1996; p. 1480.
24. Klamt, A. The COSMO and COSMO-RS solvation models. *Wiley Interdiscip. Rev. Comput. Mol. Sci.* **2018**, *8*, e1338. [CrossRef]
25. Berisha, A. Interactions between the aryldiazonium cations and graphene oxide: A DFT study. *J. Chem.* **2019**, *2019*, 5. [CrossRef]
26. Orqusha, N.; Phal, S.; Berisha, A.; Tesfalidet, S. Experimental and theoretical study of the covalent grafting of triazole layer onto the gold surface. *Materials* **2020**, *13*, 2927. [CrossRef] [PubMed]
27. Berisha, A.; Combellas, C.; Kanoufi, F.; Médard, J.; Decorse, P.; Mangeney, C.; Pinson, J. Alkyl-modified gold surfaces: Characterization of the Au–C bond. *Langmuir* **2018**, *34*, 11264–11271. [CrossRef] [PubMed]
28. Berisha, A. First principles details into the grafting of aryl radicals onto the free-standing and borophene/Ag (1 1 1) surfaces. *Chem. Phys.* **2021**, *544*, 111124. [CrossRef]
29. Lu, T.; Chen, F. Multiwfn: A multifunctional wavefunction analyzer. *J. Comput. Chem.* **2021**, *33*, 580–592. [CrossRef]
30. Humphrey, W.; Dalke, A.; Schulten, K. VMD: Visual molecular dynamics. *J. Mol. Graph.* **1996**, *14*, 33–38. [CrossRef]
31. Saby, C.; Ortiz, B.; Champagne, G.Y.; Bélanger, D. Electrochemical modification of glassy carbon electrode using aromatic diazonium salts. 1. Blocking effect of 4-nitrophenyl and 4-carboxyphenyl groups. *Langmuir* **1997**, *13*, 6805–6813. [CrossRef]
32. Braham, Y.; Barhoumi, H.; Maaref, A.; Bakhrouf, A.; Jaffrezic-Renault, N. Proteus mirabilis bacteria biosensor development based on modified gold electrode with 4-carboxyphenyl diazonium salts for heavy metals toxicity detection. *Sens. Transducers* **2014**, *27*, 29–38.
33. Liu, G.; Böcking, T.; Gooding, J.J. Diazonium salts: Stable monolayers on gold electrodes for sensing applications. *J. Electroanal. Chem.* **2007**, *600*, 335–344. [CrossRef]
34. Liu, G.; Liu, J.; Böcking, T.; Eggers, P.K.; Gooding, J.J. The modification of glassy carbon and gold electrodes with aryl diazonium salt: The impact of the electrode materials on the rate of heterogeneous electron transfer. *Chem. Phys.* **2005**, *319*, 136–146. [CrossRef]
35. Benedetto, A.; Balog, M.; Viel, P.; Le Derf, F.; Sallé, M.; Palacin, S. Electro-reduction of diazonium salts on gold: Why do we observe multi-peaks? *Electrochim. Acta* **2008**, *53*, 7117–7122. [CrossRef]
36. Pinson, J.; Podvorica, F. Attachment of organic layers to conductive or semiconductive surfaces by reduction of diazonium salts. *Chem. Soc. Rev.* **2005**, *34*, 429–439. [CrossRef]
37. Gung, B.W.; Zou, Y.; Xu, Z.; Amicangelo, J.C.; Irwin, D.G.; Ma, S.; Zhou, H.C. Quantitative study of interactions between oxygen lone pair and aromatic rings: Substituent effect and the importance of closeness of contact. *J. Org. Chem.* **2008**, *73*, 689–693. [CrossRef] [PubMed]
38. Haziri, V.; Berisha, A.; Podvorica, F.I. Electrochemical modification of platinum and glassy carbon surfaces with pyridine layers and their use as complexing agents for copper (II) ions. *Open Chem.* **2019**, *17*, 722–727. [CrossRef]
39. Jiang, D.E.; Sumpter, B.G.; Dai, S. How do aryl groups attach to a graphene sheet? *J. Phys. Chem. B* **2006**, *110*, 23628–23632. [CrossRef]
40. Berisha, A. The influence of the grafted aryl groups on the solvation properties of the graphyne and graphdiyne-a MD study. *Open Chem.* **2019**, *17*, 703–710. [CrossRef]
41. Alija, A.; Gashi, D.; Plakaj, R.; Omaj, A.; Thaçi, V.; Reka, A.; Berisha, A. A theoretical and experimental study of the adsorptive removal of hexavalent chromium ions using graphene oxide as an adsorbent. *Open Chem.* **2020**, *18*, 936–942. [CrossRef]
42. Berisha, A.; Combellas, C.; Kanoufi, F.; Decorse, P.; Oturan, N.; Médard, J.; Pinson, J. Some theoretical and experimental insights on the mechanistic routes leading to the spontaneous grafting of gold surfaces by diazonium salts. *Langmuir* **2017**, *33*, 8730–8738. [CrossRef]
43. Janssen, J.L.; Beaudin, J.; Hine, N.D.; Haynes, P.D.; Côté, M. Bromophenyl functionalization of carbon nanotubes: An ab initio study. *Nanotechnology* **2013**, *24*, 375702. [CrossRef]